G. Bitan
L. Scheibler
H. Teng
M. Rosenblatt
M. Chorev

Design and evaluation of benzophenone-containing conformationally constrained ligands as tools for photoaffinity scanning of the integrin $\alpha_V\beta_3$–ligand bimolecular interaction

Authors' affiliations:
G. Bitan, L. Scheibler,* H. Teng, M. Rosenblatt and M. Chorev,* Division of Bone and Mineral Metabolism, Charles A. Dana and Thorndike Laboratories, Department of Medicine, Beth Israel Deaconess Medical Center and Harvard Medical School, 330 Brookline Ave., Boston, MA 02215, USA.

Correspondence to:
Dr *Michael Chorev*
Beth Israel Deaconess Medical Center
330 Brookline Ave. (HIM 944)
Boston
MA 02215
USA
Tel.: 1-617-667-0901
Fax: 1-617-667-4432
E-mail: michael_chorev@hms.harvard.edu

Dates:
Received 21 May 1999
Revised 12 July 1999
Accepted 8 August 1999

To cite this article:
Bitan, G., Scheibler, L., Teng, H., Rosenblatt, M. & Chorev, M. Design and evaluation of benzophenone-containing conformationally constrained ligands as tools for photoaffinity scanning of the integrin $\alpha_V\beta_3$–ligand bimolecular interaction.
J. Peptide Res., 2000, **55**, 181–194.
*Both authors contributed equally to this work.

ISSN 1397–002X

Abstract: Integrins are cell-surface adhesion molecules involved in mediating cell–extracellular matrix interactions. High-resolution structural data are not available for these heterodimeric receptors. In order to generate tools for photoaffinity scanning of the RGD-binding site of human integrin $\alpha_V\beta_3$, new conformationally constrained ligands were designed. The ligands were based on five different cyclic peptidic or peptidomimetic scaffolds with high affinity for $\alpha_V\beta_3$. A single photoreactive group (a benzophenone moiety) was introduced at different positions relative to the RGD triad. In addition, an ^{125}I or a biotin group was introduced as a reporting tag. Twenty-four cyclic ligands were prepared and their binding affinity for $\alpha_V\beta_3$ was determined. In most cases, the modifications resulted in a 5- to 500-fold decrease in affinity relative to the unmodified scaffold. Analogs representing three of the five families were screened for their cross-linking efficiency. Ligands with submicromolar affinities cross-linked efficiently and specifically to the integrin receptor, whereas ligands with weaker affinities gave specific cross-linking, but with lower efficiency. Almost all of the screened ligands cross-linked predominantly to the β_3 subunit.

Abbreviations: Abba, 2-(2′-aminobenzoyl)benzoic acid; ACN, acetonitrile; Ahx, 6-aminohexanoyl/6-aminohexanoic acid; Alloc, Allyloxycarbonyl; Apr, L-4-aminoproline; BH, Bolton-Hunter reagent; Bpa, L-4-benzoylphenylalanine; BSA, bovine serum albumin; DAST, (diethylamino)sulfur trifluoride; DCC, *N*,*N*′-dicyclohexylcarbodiimide; DCM, dichloromethane; Dde, 1-(4,4-dimethyl-2,6-dioxocyclohexylidene)ethyl; DIC, *N*,*N*′-diisopropylcarbodiimide; DMF, *N*,*N*-dimethylformamide; Dmt, L-5,5-dimethylthiazolidinecarboxylic acid; Dpr, L-1,3-diaminopropanoic acid; ECM, extracellular matrix; EtOAc, ethyl acetate; Fmoc, 9-fluorenylmethyloxycarbonyl; HATU, 2-[1H-(7-azabenzotriazol-1-yl)]-1,1,3,3-tetramethyluronium

hexafluorophosphate; HBTU, 2-(1H-benzotriazol-1-yl)-1,1,3,3-tetramethyluronium hexafluorophosphate; Hcy, homocysteine; HOBt, *N*-hydroxybenzotriazole; LIBS, ligand-induced binding site; Mpa, 3-mercaptopropanoic acid; NHS, *N*-hydroxysuccinimide; NMP, *N*-methylpyrrolidone; Pbf, 2,2,4,6,7-pentamethyldihydrobenzofuran-5-sulfonyl; pBz$_2$, 4-benzoylbenzoyl; pBz$_2$OH, 4-benzoylbenzoic acid; PEG, polyethyleneglycol; *p*MBHA, 4-methylbenzhydrylamine; PTH, parathyroid hormone; PyBOP, benzotriazole-1-yloxytrispyrrolidinophosphonium hexafluorophosphate; SPPS, solid-phase peptide synthesis; TBS, Tris-buffered saline; TFFH, tetramethylfluoroformamidinium hexafluorophosphate; Tle, *tert*-leucine; Trt, trityl; Xan, xanthyl.

Generating a high-resolution three-dimensional structure of a protein is in many cases a key step toward understanding its biological role. X-ray crystallography and NMR spectroscopy investigations have generated a wealth of invaluable structural data for numerous proteins, including enzymes, antibodies and other water-soluble globular proteins. However, both X-ray crystallography and NMR are of limited use for structural studies of highly hydrophobic membrane-embedded proteins. In addition, very large molecules may be unsuitable for detailed structural studies, especially by NMR. It is therefore not surprising that out of more than 7000 protein structures stored in the Brookhaven National Laboratories Protein Data Bank, only 1% are membrane-bound proteins (1). Moreover, there are entire families of membrane-bound proteins for which no high resolution structures are available. Examples of such biologically important families are G-protein-coupled receptors, ion-channels and adhesion molecules.

To avert the difficulties encountered in direct structural investigation of the interaction between membrane-bound receptors and their ligands, indirect methods, such as mutational analysis, generation of deletion-containing mutant receptors or receptor chimeras, and antibody mapping have been used. In addition, indirect data have been obtained using structure–activity relationship studies of ligands alone. In some cases, direct information about the receptor molecule (but not the receptor–ligand complex) has been obtained by NMR or X-ray investigations of segments or modules of the receptor (2–4).

Complementary to these indirect approaches is photoaffinity cross-linking, a method which provides direct information about the binding surface by identifying contact sites between ligands (which are modified to incorporate a photoreactive group) and their receptors (5). By carefully designing bioactive ligands that contain both a single photoreactive moiety positioned at discrete positions in the ligand and a reporting 'tag', a topological map of the ligand–receptor interface can be generated (6). The resolution offered by this methodology is not as high as that of NMR or X-ray crystallography, yet in many cases, and membrane-bound receptors is one of them, photoaffinity scanning is the best tool available for direct structural investigation of the ligand–receptor interface.

Integrins are membrane-bound cell-surface adhesion molecules involved in cell–extracellular matrix (ECM) and cell–cell interactions (7, 8). These heterodimeric glycoproteins are composed of two subunits, α and β, both characterized by a large N-terminal extracellular component, a transmembrane domain and a short C-terminal intracellular tail. Currently, there are 23 known integrins based on combinations of 17 α and 8 β subunits (9).

Many integrins recognize the arginyl-glycyl-aspartyl (RGD) motif, found in various ECM proteins and disintegrins as their primary binding motif (10). Among them, and of special interest for us, is the $\alpha_V\beta_3$ integrin (vitronectin receptor), which binds several RGD-containing proteins, including fibronectin, fibrinogen, vitronectin, von Willebrand factor, bone sialoprotein and osteopontin, as well as many disintegrins and small RGD-containing peptides. The various physiological processes in which $\alpha_V\beta_3$ may be involved include angiogenesis (11), apoptosis (12) and bone resorption (13). $\alpha_V\beta_3$ is the most abundant integrin in osteoclasts, the multinucleated cells responsible for bone resorption. Interaction between $\alpha_V\beta_3$ and the bone matrix may serve to form the intimate cell–matrix 'tight seal' essential for the resorptive process (14). Therefore, inhibition of $\alpha_V\beta_3$ function may provide a novel mechanism-based approach for the treatment of diseases associated with increased bone resorption such as osteoporosis (13, 15).

Rational design of antagonists of integrin receptors will benefit from a detailed understanding of the structure of the integrin–ligand complex. Being large, membrane-embedded proteins, structure–function information about integrins has been generated almost entirely by indirect methods such as mutational analysis (16–18), creation of receptor chimeras (19, 20) and deletion-containing mutants (21), biological characterization of peptides derived from putative binding sites (22) and generation of activating (23) or inhibitory (22) antibodies.

Early attempts to elucidate the nature of the bimolecular interaction between the β_3-containing integrins, $\alpha_V\beta_3$ and $\alpha_{IIb}\beta_3$, and radioiodinated RGD-containing ligands by cross-linking methods employed either homobifunctional

chemical cross-linkers (24) or arylazide-based photoaffinity agents (25, 26). Although the predominant cross-linking occurred with the β_3 subunit, only large segments within the receptor, such as the sequences 109–171 (24) or 217–302 (26) in $\alpha_{IIb}\beta_3$ and 61–203 in $\alpha_V\beta_3$ (25) could be assigned.

Recently, benzophenone-based photoaffinity scanning has emerged as a preferred method for mapping the bimolecular interfaces of ligand–receptor complexes. The advantageous properties of the benzophenone moiety, compared with arylazide and other photoreactive moieties (27), include low reactivity with water, favorable photokinetics with high cross-linking specificity and efficiency, and convenience in synthesis, purification and handling. These properties have been exploited in recent years for probing the interaction between substrates and enzymes, such as steroid 5-α-reductase (28) and glutathione *S*-transferase (29), as well as other bimolecular interactions involving ligands and membrane-bound receptors, such as the neurokinin-1 receptor (30, 31), the parathyroid hormone (PTH)/PTH-related protein receptor (6, 32, 33), the urokinase-type plasminogen activator receptor (34), the angiotensin AT4 receptor (35) and the secretin receptor (36).

In this work we set out to develop biologically active RGD-based ligands which contain a benzophenone moiety placed in several different positions relative to the RGD pharmacophore. These photoreactive ligands will serve as tools for mapping the bimolecular interface of the $\alpha_V\beta_3$–RGD-containing ligand complex. We selected as parent molecular scaffolds small cyclic peptides (or peptidomimetics) known to posses high affinity for $\alpha_V\beta_3$. These photoreactive ligands must also incorporate a reporting tag, e.g. a radionucleide or a fluorescent moiety to enable monitoring of the isolation and purification of the photoconjugate and its subsequent fragmentation. Based on our in-house database and a literature survey, five different conformationally constrained RGD-based $\alpha_V\beta_3$ antagonists were selected as candidate scaffolds for the incorporation of a benzophenone group and a 'tag' moiety: *cyclo* Ac-[Cys-Asn-Dmt-Arg-Gly-Asp-Cys]-OH, 1, IC_{50} = 50 nM, *cyclo*[Mpa-Arg-Gly-Asp-Asp-Tle-Cys]-OH, 2, IC_{50} = 6 nM (37), *cyclo*[-Arg-Gly-Asp-D-Phe-Val-], 3, IC_{50} = 10 nM (38), *cyclo*[-Arg-Gly-Asp-Ser-Pro-Gly-], 4, IC_{50} = 10 nM (39) and the peptidomimetic antagonist 5 (Fig. 1), IC_{50} = 3.5 nM (40).

The utilization of a first bioactive photoreactive ligand generated in this work has lead to the elucidation of the first small 'contact domain' between the C-terminus of scaffold 1 and a 20-amino acid sequence in the N-terminus of the β_3 subunit (41).

Experimental Procedures

General

Boc-Cys(4-MeBzl)-OH, Boc-Asn(Xan)-OH, Boc-Arg(Tos)-OH, Boc-Asp(cHex)-OH, *p*MBHA resin and 1.0 M DCC and HOBt solutions were purchased from Applied Biosystems (Foster City, CA). Dmt and Boc-Dmt were purchased from Schweizerhall (Piscataway, NJ). Boc-Tle and DAST were purchased from Fluka (Milwaukee, WI). Fmoc-Arg(Pbf)-OH was purchased from Nova Biochem (San Diego, CA). All other Fmoc-protected amino acids, as well as Boc-Hcy(MeBzl)-OH, Boc-Bpa-OH and Fmoc-Gly-Sasrin resin, were from Bachem (Torrance, CA). H-Gly-2Cl-Trt resin was from Advanced ChemTech (Louisville, KY). HBTU was purchased from Quantum Biotechnologies (Montreal, Canada). HATU was purchased from PerSeptive (Framingham, MA). HPLC grade DMF, NMP, ACN, MeOH and DCM were from Burdrick & Jackson (Muskegon, MI). Biotin was purchased from Sigma (St. Louis, MO). EZ-Link™-Sulfo-NHS-LC-Biotin and biotin-NHS were from Pierce (Rockford, Il). Succinimidyl α-carboxyl-ω-Boc-amino-polyethyleneglycol was purchased from Shearwater Polymers (Huntsville, AL). Other reagents and solvents were from Aldrich (Milwaukee, WI). Analytical, semi-preparative and preparative RP-HPLC separations were performed using HPLC systems from Waters (Milford, MA) as described previously (42). Amino acid analysis was performed at the Biopolymers Laboratory of Brigham and Women's Hospital, Boston, MA. Mass-spectra were acquired in house or in the laboratories of Drs Andrew Tyler, Chemistry Department, Harvard University, Cambridge, MA and Jim Lee, Dana-Farber Cancer Research Institute, Boston, MA.

Peptide synthesis

tert-Butoxycarbonyl (Boc) strategy, chain elongation

Automated solid-phase peptide synthesis (SPPS) employing Boc strategy with an Applied Biosystems ABI 430 synthesizer (42) on 4-methylbenzhydrylamine (*p*MBHA) resin was used for the synthesis of all disulfide-containing peptides (series **1** and **2** except for **1j**). In the synthesis of **1** and its analogs the coupling of N^{α}-tert-butoxycarbonyl-N^{γ}-xanthylasparagine [Boc-Asn(Xan)-OH] to 5,5-dimethylthiazolidinecarboxylic acid (Dmt) was performed manually twice for 3 h with 2-[1H-(7-azabenzotriazol-1-yl)]-1,1,3,3-tetramethyluronium hexafluorophosphate (HATU) as the coupling reagent. Completion of the coupling was verified by amino acid analysis, and then the synthesis was continued automati-

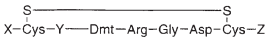

Peptide	X	Y	Z	IC_{50} (μM)
1	Ac	Asn	COOH	0.05±0.02
1a	BH	Asn	Bpa-$CONH_2$	0.3
1b	I-BH-Ahx	Asn	Bpa-$CONH_2$	0.7±0.4
1c	I-BH-PEG	Asn	Bpa-$CONH_2$	0.3±0.03
1d	biotin-Ahx	Asn	Bpa-$CONH_2$	0.5±0.05
1e	pBz_2	Asn	N^{ε}-(I-BH-Ahx)Lys-$CONH_2$	1.0±0.2
1f	pBz_2	Asn	N^{ε}-(biotin-Ahx)Lys-$CONH_2$	0.3±0.05
1g	pBz_2-Ahx	Asn	N^{ε}-(biotin-Ahx)Lys-$CONH_2$	1.3±0.6
1h	biotin-Ahx	N^{ε}-(pBz_2)Lys	$CONH_2$	4.5±0.5
1i	I-BH-Ahx	N^{ε}-(pBz_2)Lys	$CONH_2$	5.6±0.3
1j	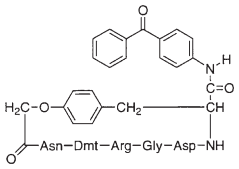			>100

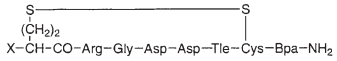

Peptide	X	IC_{50}(μM)
2	H	0.006*
2a	biotin-NH	2.5±0.2
2b	biotin-Ahx-NH	3.5±0.5
2c	I-BH-NH	0.3±0.05

*See reference (37)

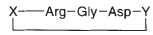

Peptide	X	Y	IC_{50}(μM)
3	Val	D-Phe	0.01†
3a	Bpa	D-Tyr	0.1
3b	N^{ε}-(pBz_2)Lys	D-Tyr	0.2
3c	Tyr	N^{ε}-(pBz_2)-D-Lys	0.05±0.03
3d	N^{ε}-(pBz_2)-D-Lys	Tyr	0.4
3e	D-Tyr	Bpa	0.3
3f	D-Tyr	N^{ε}-(pBz_2)Lys	1.3

† See reference (38)

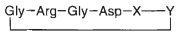

Peptide	X	Y	IC_{50}(μM)
4	Ser	Pro	0.01‡
4a	N^{γ}-(pBz_2)-Dpr	N^{δ}-I-BH-Apr	5.1
4b	N^{γ}-I-BH-Dpr	N^{d}-(pBz_2)-Apr	3.7
4c	N^{γ}-(pBz_2)-Dpr	N^{δ}-I-BH-Ahx-Apr	7±2
4d	N^{γ}-I-BH-Ahx-Dpr	N^{d}-(pBz_2)-Apr	6±3

‡ See reference (39)

Peptide		IC_{50}(μM)
5	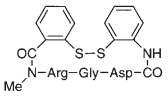	0.01§
5a	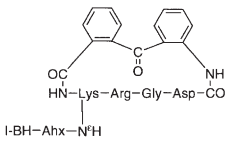	5.9±0.5

§ See reference (40)

Figure 1. Structures and IC_{50} values of cyclic RGD-containing peptide scaffolds and the photoreactive derivatives reported in this work. Ligands were screened for binding to $\alpha_V\beta_3$ by one experiment performed in triplicates. Only ligands which were eventually selected for cross-linking experiments were further characterized by three independent experiments.

cally. Coupling of biotin to the N-terminus in the synthesis of peptide **2a** was performed manually with 2-(1H-benzotriazol-1-yl)-1,1,3,3-tetramethyluronium hexafluorophosphate (HBTU) as the coupling reagent and *N*,*N*-dimethylformamide (DMF) as a solvent. Since biotin has low solubility in DMF, the coupling time was extended to 16 h allowing the biotin to gradually dissolve in the reaction mixture.

Boc strategy, cleavage and cyclization

Peptides of series **1** and **2** were cleaved from the resin by HF with 5% thioanisol as a scavenger. The reaction was performed at 0°C for 75 min. Disulfide bond formation was performed using I_2 in acetic acid as described previously (43).

9-Fluorenylmethyloxycarbonyl (Fmoc) strategy, chain elongation

Peptide **1j**, peptidomimetic **5a** and analogs of series **4** were synthesized on Fmoc-Gly-Sasrin resin by manual Fmoc chemistry using 1.5 eq of Fmoc protected amino acid, 3 eq of *N*,*N*-diisopropylethylamine (DIEA) and 1.5 eq. of benzotriazole-1-yloxytrispyrrolidinophosphonium hexafluorophosphate (PyBOP). In the synthesis of peptide **1j** the Asn and Dmt residues were introduced as the preprepared Fmoc-Asn(Trt)-Dmt-OH dipeptide **14** (see below). Similarly, in the synthesis of analog **5a** the Asp and 2-(2′-aminobenzoyl)benzoic acid (Abba) residues were introduced as the preprepared Fmoc-Asp(*t*-Bu)-Abba-OH dipeptide **15** (see below).

Head-to-tail cyclic pentapeptides (series **3**) were prepared on H-Gly-2Cl-Trt resin according to the method of Wermuth *et al.* (44). In the synthesis of peptides **3a** and **3e** the coupling of Fmoc-4-benzoylphenylalanine (Fmoc-Bpa) was difficult and was carried out with HATU as the coupling reagent. It required two recoupling cycles for completion. The Lys side-chain in peptides **3b**, **3c**, **3d** and **3f** was protected by 1-(4,4-dimethyl-2,6-dioxocyclohexylidene)ethyl (Dde).

Fmoc strategy, cleavage and cyclization

Peptide **1j**, peptidomimetic **5a** and analogs of series **4** were cleaved from the solid support by treatment with 1% trifluoroacetic acid (TFA) in dichloromethane (DCM) (10 × 3 min). The solution containing the crude cleaved peptide was immediately neutralized with pyridine. Evaporation of the solvent and RP-HPLC purification yielded the linear protected peptides. For cyclization of **1j** 100 mg (64 mmol) of the protected linear peptide were dissolved and stirred in 100 mL DMF with 2 eq. of DIEA and 1.1 eq. of PyBOP. After 1 h, the solvent was removed under reduced pressure and the remaining oil was taken up in a minimal amount of MeOH. Precipitation with ether yielded 83 mg (84%) of the cyclic peptide. The protected cyclic peptide was treated without further purification with a cleavage cocktail comprised of TFA/*p*-cresol/ansiol/phenol/thioanisol/triethylsilane/water 100 : 10 : 10 : 10 : 20 : 1 : 1 (v/v). After 45 min the solution was evaporated under reduced pressure and the peptide was precipitated with ice-cold ether and purified by RP-HPLC. Peptides of series **4** were cleaved and cyclized using the same methods. Cleavage and cyclization of peptidomimetic **5a** and peptides from series **3** were performed according to the procedure of Wermuth *et al*. (44).

Post synthetic modifications

Dde deprotection

The Dde group was removed by treatment with 2% N_2H_4 in DMF for 15 min at room temperature. The reaction mixture was neutralized with acetic acid and the solvent was evaporated under reduced pressure. The crude mixture was re-dissolved in 10 mM AcOH and lyophilized.

Allyloxycabonyl (Alloc) deprotection (45)

The Alloc group was removed by treatment of a solution of the protected cyclic peptide (50 mg) with 1 mL glacial AcOH, 1–3 mg of $PdCl_2$ $(PPh_3)_2$ and 4 eq. of Bu_3SnH in 30 mL DCM under N_2 for 1 h at ambient temperature. The orange solution was concentrated and the crude residue was dissolved in MeOH and precipitated with ice-cold ether. The precipitate was dissolved in 50% acetic acid, filtered and lyophilized.

Introduction of *N*-biotinylaminohexanoyl (biotin-Ahx), biotin and α-carboxy-N$^{\omega}$-Boc-aminopolyethyleneglycol

Peptides **1d**, **1e**, **1f**, **1i** and **2b** were modified after cleavage from the resin and HPLC purification using EZ-Link™-Sulfo-NHS-LC-Biotin (10 eq. in DMF, overnight in the presence of 10 eq. DIEA). Peptide **1c** was modified by the same way with Boc-NH-PEG-CO_2-NHS (M_r 3400). The Boc group was then removed by stirring with TFA/DCM/anisol 52 : 43 : 5 (v/v) for 30 min. The modified peptides were re-purified by semi-preparative HPLC.

Introduction of Ahx spacer

Boc-Ahx was activated as the *N*-hydroxysuccinimide (NHS) ester by reaction with 1.1 eq. of NHS, 1,3-dicyclohexylcarbodiimide (DCC) and DIEA in ether for 2 h. The 1,3-dicyclohexylurea was filtered out and the ether was evaporated. The NHS ester was dissolved in DMF and 0.1 eq. of peptide was added. The reaction was performed at ambient temperature and was monitored by HPLC. After completion of the coupling (2–3 h) the solvent was evaporated and the Boc group was removed by stirring with TFA/DCM/anisol 52 : 43 : 5 (v/v) for 30 min. The modified peptide was re-purified by HPLC.

Introduction of 4-benzoylbenzoic acid

p-Bz2OH was preactivated with 1 eq. of 1,3-diisopropylcarbodiimide (DIC) in DMF for 30 min and then added to a solution of 0.1 eq. of the peptide bearing a free NH_2 group along with 1 eq. of DIEA. The mixture was stirred at room temperature for 2 h. Completion of the coupling was monitored by HPLC (2–3 h), and the solvent was then evaporated under reduced pressure. The crude modified peptides were re-purified by HPLC.

Deprotection of side-chain protecting groups in Fmoc strategy

The 2,2,4,6,7-pentamethyldihydrobenzofuran-5-sulfonyl (Pbf), Boc and *t*-butyl protecting groups were deprotected from the side-chains of the Arg, Asp, Lys and Tyr residues by treatment with TFA and scavengers as described (44).

HPLC purification

All of the peptides were purified by preparative or semi-preparative HPLC using the eluent system A, 0.1% TFA in ddH_2O; B, 0.1% TFA in ACN, and monitoring at 220 nm (42). Typically the flow rates were 20 mL/min for semi-preparative separations and 70 mL/min for preparative separations. All peptides were > 97% pure before further use. Their integrity was confirmed by mass-spectroscopy and amino acid analysis (Table 1).

Introduction of ^{125}I-Bolton-Hunter

A 15 nmol aliquot of a precursor peptide bearing a free NH_2 group dissolved in 100 mL 0.1 M sodium phosphate buffer pH 8.0 was incubated with 1 mCi of ^{125}I-Bolton-Hunter reagent at 0°C for 2 h and then for 16 h at ambient

Table 1. **Physical properties of the photoreactive ligands**

Peptide	Amino acid analysis[a]	Mass spectrometry[b]
1a	Asx-1.97, Gly-1.04, Arg-0.99	1206 (1206.4)
1b	Asx-2.07, Gly-1.03, Arg-0.90	1397 (1397.7)
1c	Asx-2.06, Gly-1.08, Arg-0.86	1445 (1444.5)
1d	Asx-2.04, Gly-1.10, Arg-0.97	4500–4700 (≈ 4600)[c]
1e	Asx-2.11, Gly-1.02, Lys-1.02, Arg-0.86	1531.0 (1530.5)
1f	Asx-2.00, Gly-1.05, Lys-1.05, Arg-0.90	1371 (1369.6)
1g	Asx-2.02, Gly-1.03, Lys-1.04, Arg-0.91	1483 (1482.8)
1h	Asx-1.01, Gly-1.11, Lys-1.01, Arg-0.88	1369.1 (1367.8)
1i	Asx-1.03, Gly-1.16, Lys-0.85, Arg-0.96	1417.0 (1414.8)
1j	Asx-2.05, Gly-1.06, Arg-0.88	986 (986.1)
2a	Asx-2.02, Gly-0.99, Arg-0.99	1269 (1269.5)
2b	Asx-2.02, Gly-0.99, Arg-0.99	1382 (1382.6)
3a	Asx-1.05, Gly-1.00, Tyr-0.96, Arg-1.00	743 (742.8)
3b	Asx-1.06, Gly-1.02, Tyr-0.97, Lys-1.00, Arg-0.95	828 (828.9)
3c	Asx-1.02, Gly-1.01, Tyr-0.95, Lys-1.01, Arg-1.00	828 (828.9)
3d	Asx-1.04, Gly-1.03, Tyr-0.95, Lys-1.04, Arg-0.95	828 (828.9)
3e	Asx-0.95, Gly-1.01, Tyr-1.01, Arg-1.02	743 (742.8)
3f	Asx-1.02, Gly-1.00, Tyr-0.95, Lys-1.01, Arg-0.92	828 (828.9)
4a	Asx-0.95, Gly-2.10, Arg-0.95	941 (940.0)
4b	Asx-0.99, Gly-2.03, Arg-0.97	941 (940.0)
4c	Asx-1.01, Gly-2.05, Arg-0.94	1054 (1053.1)
4d	Asx-1.01, Gly-2.03, Arg-0.95	1054 (1053.1)
5a	d	1067 (1066.9)

a. Natural amino acids only, not including Cys. b. The calculated mass is given in parenthesis. c. The mass spectrum showed a distribution of masses separated by 44 mass units and centered around 4600. d. No amino acids were observed, presumably due to decomposition of compound **5a** during hydrolysis.

temperature. The radiolabeled peptide was isolated by a RP-HPLC using a Nova-Pak C18 column (3.9–150 mm; Waters, Milford, MA) with the same solvent system as above. Purification was carried out using a suitable linear gradient during 30 min at a flow rate of 1 mL/min, monitored at 220 nm. The radioactive peak was collected (0.5 min/fraction) and the radioactivity in each fraction was monitored by a γ-radiation counter. The fractions containing the radioactive peak were pooled and stored at –80°C.

Synthesis of amino acid derivatives and dipeptides

N^{α}-Boc-tyrosine 4-benzoylanilide, **6**

DCC (403 mg, 1.96 mmol) and 4-aminobenzophenone (350 mg, 1.78 mmol) were added to a solution of Boc-Tyr-OH (500 mg, 1.78 mmol) in a mixture of DCM (10 mL) and DMF (0.5 mL). After stirring for 2 h, the solution was filtered and the solvents were removed *in vacuo*. The residue was taken up in ether (35 mL) and washed consecutively with 10% citric acid (3 × 50 mL) and brine (3 × 50 mL). The organic phase was dried over $MgSO_4$ and the solvent was evaporated. Yield: 790 mg (96%). TLC-R_f = 0.35 (hexane/EtOAc 2 : 1), HPLC-R_t = 16.8 min (25–100% B in 30 min), MS (FAB+) = 461, M_r = 460.52. ^{1}H NMR (DMSO-d_6, 500 MHz, d): 10.4 (s, 1H), 7.5–7.8 (m, 10H), 7.2 (m, 3H), 6.7 (d, 2H), 4.3 (m, 1H), 2.8 (m, 2H), 1.3 (s, 9H).

O-(*t*-butoxycarbonylmethyl)-N^{α}-Boc-tyrosine 4-benzoylanilide, **7**

K_2CO_3 (2.5 g, 18 mmol) was added to a solution of **6** (500 mg, 1.09 mmol) and *t*-butyl bromoacetate (2 mL, 13 mmol) in 50 mL of acetone. The mixture was refluxed overnight and the solvent was evaporated *in vacuo*. The remaining oil was taken up in ether (100 mL) and washed with water (75 mL), 5% $NaHCO_3$ (3–75 mL), 10% citric acid (3–75 mL) and brine (3–50 mL). The organic phase was dried over $MgSO_4$, the solvent was evaporated and the residue was purified by silica column chromatography eluting with hexane/EtOAc – 3 : 1. Yield: 400 mg (64%). TLC-R_f = 0.28

(hexane/EtOAc 3 : 1). HPLC-R_t = 22.0 min (25–100% B in 30 min), MS (FAB+): 597 (M+Na), M_r = 574.66. ^{1}H NMR (DMSO-d_6, 500 MHz, d): 10.4 (s, 1H), 7.5–7.8 (m, 10H), 7.2 (m, 3H), 6.7 (d, 2H), 4.3 (m, 1H), 2.8 (m, 2H), 1.3 (s, 9H).

O-(carboxymethyl)-N$^\alpha$-Fmoc-tyrosine 4-benzoylanilide, **9**

The Boc and *t*-butyl ester groups were removed from 400 mg of **7** by treatment with a cocktail of TFA/*p*-cresol/ansiol/phenol/water, 50 : 5 : 5 : 5 : 1 for 1 h. The solution was evaporated and the remaining oil was taken up in a small amount of MeOH. Precipitation with ice-cold ether yielded 275 mg (95%) of *O*-(carbxymethyl)-tyrosine 4-benzoylanilide (**8**). HPLC-R_t = 17.4 (5% B to 100% B in 38 min), MS (FAB+): 419, M_r = 418.44. ^{1}H NMR (DMSO-d_6, 500 MHz, d): 10.4 (s, 1H), 7.5–7.8 (m, 10H), 7.2 (m, 3H), 6.7 (d, 2H), 4.3 (m, 1H), 2.8 (m, 2H), 1.3 (s, 9H). **8** was dissolved in a 30-mL of 1 : 2 water/ACN mixture, to which triethylamine (280 mL, 2 mmol) and Fmoc-NHS (310 mg, 0.80 mmol) was added. The reaction mixture was stirred at room temperature overnight, and then diluted with 30 mL of water and washed successively with hexane (3 × 50 mL) and a mixture of hexane/ether 7 : 3 (3 × 50 mL). The aqueous solution was acidified with concentrated HCl. The Fmoc-protected amino acid precipitated spontaneously and was collected by filtration to give 415 mg (97%). HPLC-R_t = 28.1 min (5% B to 100% B in 38 min), MS (FAB+): 640 (M+), M_r = 640.68. ^{1}H NMR (DMSO-d_6, 500 MHz, d): 10.4 (s, 1H), 7.5–7.8 (m, 10H), 7.2 (m, 3H), 6.7 (d, 2H), 4.3 (m, 1H), 2.8 (m, 2H), 1.3 (s, 9H).

N$^\alpha$-Fmoc-S-*cis*-4-Alloc-aminoproline, **10**

A 378 mg (1.55 mmol) aliquot of N$^\alpha$-Boc-S-*cis*-4-aminoproline methyl ester (11, 46, 47) were dissolved in 10 mL DMF and stirred with DIEA (530 μL, 3.1 mmol) and allyl chloroformate (197 μL, 1.86 mmol) for 2 h at ambient temperature. The solvent was then removed *in vacuo* and the remaining oil was taken up in 40 mL EtOAc and washed with 5% $KHSO_4$ (3 × 50 mL), 10% citric acid (3 × 50 mL) and 50 mL brine. The organic phase was dried over $MgSO_4$ and evaporated to dryness to give N$^\alpha$-Boc-S-*cis*-4-Alloc-aminoproline methyl ester, **12**. The methyl ester was removed to yield N$^\alpha$-Boc-S-*cis*-4-Alloc-aminoproline, **13** by stirring with 15 mL of 2 : 1 1,4-dioxane/2 N NaOH mixture for 2 h. The solvents were removed *in vacuo* and the residue was taken up in 50 mL EtOAc and washed with 1 N $KHSO_4$ (3 × 50 mL) and 50 mL of brine. The organic phase was dried over $MgSO_4$ and the solvent was evaporated. The Boc-protecting group was removed from 13 by reaction with 10 mL 1 : 1 TFA/DCM for 1 h at ambient temperature. The mixture was evaporated and the residue was dissolved in 30 mL 1 : 2 water/acetonitrile. The Fmoc-protecting group was introduced by applying the same protocol as for compound **8** using 520 mg Fmoc-NHS (1.54 mmol) and 550 mL DIEA (3.20 mmol). Compound **10** was purified by flash chromatography eluting with EtOAc/hexane/AcOH 40 : 60 : 1. Yield: 410 mg (61%), TLC-R_f = 0.43 (EtOAc/hexane/AcOH 40 : 60 : 1), HPLC-R_t = 15.5 min, MS (FAB+) = 437 (M+), M_r = 436.46, ^{1}H NMR (DMSO-d_6, 500 MHz, d): 7.3–7.9 (m, 8H), 5.9 (m, 1H), 5.2 (dd, 2H), 4.5 (d, 2H), 4.0–4.4 (m, 5H), 3.7 (m, 1H), 3.1 (m, 1H), 2.9 (d, 1H), 2.6 (m, 1H), 1.8 (m, 1H)

Fmoc-Asn(Trt)-Dmt-OH, **14**

A 270 μL (2.00 mmol) quantity of (diethylamino)sulfur trifluoride (DAST) (48) was added to a solution of 1.00 g Fmoc-Asn(Trt)-OH (1.68 mmol) in 60 mL $CHCl_3$. The solution was stirred for 10 min and then washed with ice-cold water (2 × 100 mL). The organic phase was dried over $MgSO_4$ and the solvent was removed *in vacuo*. Recrystallization from $CHCl_3$/hexane yielded 940 mg (94%) of Fmoc-Asn(Trt)-F (**15**). A 300 mg (0.50 mmol) sample of **15** was stirred together with 260 μL of DIEA (1.5 mmol) and 97 mg of H-Dmt-OH (0.60 mmol) in dry DMF for 12 h. The solvent was then removed *in vacuo* and the remaining oil was taken up in 30 mL EtOAc. The organic solution was washed with 10% citric acid (3 × 20 mL) and brine (3 × 20 mL), and dried over $MgSO_4$. Evaporation of the solvent gave 351 mg (95%) of **13**. HPLC-R_t = 25.1 min (25–100% B in 30 min) MS (FAB+): 740 (M+), M_r = 739.88.

Fmoc-Asp(*t*-Bu)-Abba-OH, **16**

A 1.88 g (4.57 mmol) aliquot of Fmoc-Asp(*t*-Bu)-OH was activated as the corresponding amino acid fluoride by reaction with 1.14 g (4.57 mmol) tetramethylfluoroformamidinium hexafluorophosphate (TFFH) (49) and 1.59 mL (4.57 mmol) DIEA in 20 mL DCM for 30 min at ambient temperature. One gram (4.15 mmol) of Abba was added and the mixture was stirred for 2 h at ambient temperature. The solvent was evaporated and the residual oil was purified by preparative HPLC. Yield: 450 mg (17%). HPLC-R_t = 27.2 min (20% B to 80% B in 30 min) MS (ESI): 635.1 (M+), M_r = 634.67.

Purification of integrin $\alpha_V\beta_3$

Recombinant human integrin $\alpha_V\beta_3$ overexpressed in HEK 293 cells was purified using monoclonal antibody LM609 affinity column as described (50).

Integrin binding assay

The affinity of the peptides for purified integrin $\alpha_V\beta_3$ was measured in a radioreceptor binding assay by competition with ^{125}I-echistatin as described (50). Representative binding curves for each analog series are presented in Fig. 2.

Cross-linking of biotin-tagged peptides to purified $\alpha_V\beta_3$

Aliquots (100 pmol) of peptide and purified $\alpha_V\beta_3$ receptor were diluted into 250 mL of TBS (25 mM Tris–HCl, pH 7.5, 150 mM NaCl, 1 mM $CaCl_2$, 1 mM $MgCl_2$) with or without the presence of a competitive inhibitor (1 nmol of peptide **1**) in a 24-well plastic plate. The mixture was incubated for 1 h at room temperature and then irradiated by UV light at 365 nm in a Stratalinker 2400 cross-linker (Stratagen, La Jolla, CA) for 1 h at 4°C. Excess ligand was removed by ultrafiltration using Microcon-50 (Amicon, Beverly, MA) and the samples were analyzed by SDS–PAGE/Western blot. Electrophoretic analyses were performed using 7.5% (w/v) polyacrylamide gels. Western blot was performed using the CAPS buffer system (51) at 200 mA for 40 min. The bands were visualized using either Avidin-HRP or Amplified Alkaline Phosphatase Immun-Blot Kits (Bio-Rad, Hercules, CA) according to the manufacturer's instructions.

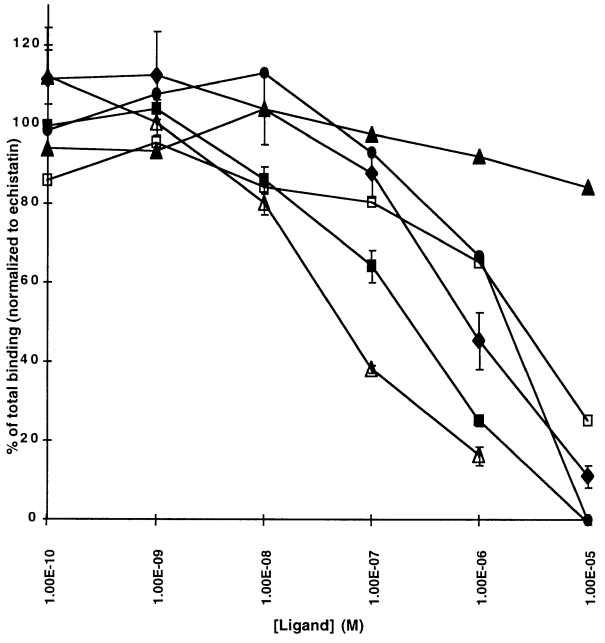

Figure 2. Binding competition curves of representative cyclic RGD-containing photoreactive ligands. ^{125}I-echistatin was used as a radioactive tracer and nonlabeled echistatin was used as a control in all assays which were performed as described in the Experimental Procedures. Key **1b** (◆), **1e** (■), **1j** (▲), **2a** (□), **3c** (△), **4b** (•).

Photoaffinity cross-linking of ^{125}I-tagged peptides to HEK 293 cells overexpressing human integrin $\alpha_V\beta_3$

Confluent cells grown in 24-well plates from Corning (Corning, NY) were incubated for 1 h at room temperature with 10^6 c.p.m. (≈ 0.2 pmol) of ^{125}I-labeled peptide diluted in serum-free medium [Before addition of ligand the medium containing 10% fetal bovine serum was replaced by serum-free medium. However, residual amounts of BSA from the serum were present in most experiments as evident by a nonspecific band at 66 kDa (Fig. 6).], with or without the presence of a competitive inhibitor, in a final volume of 250 μL/well. Following 30 min UV irradiation at 365 nm as described above the cells were washed twice with ice-cold PBS and incubated for 1 h with 300 μL sample buffer (0.06 M Tris–HCl, pH 6.8, 2% SDS, 10% glycerol, 0.025% Bromophenol Blue) at room temperature. Aliquots (50 μL) were analyzed by SDS–PAGE/autoradiography. Electrophoretic analyses were performed using 7.5% (w/v) polyacrylamide gels. Appropriate molecular mass markers (Amersham) were included in each gel. Gels were dried and exposed to X-ray films (X-omat, Kodak) with intensifying screens (XAR-5, Kodak).

Results

Preparation and binding affinity of cyclic heptapeptide/octapeptide analogs of 1

Initially, a Bpa residue was incorporated at the C-terminus of scaffold **1**, whereas 3-(4′-hydroxyphenyl)propanoic acid (Bolton-Hunter reagent, BH) was coupled at the N-terminus to form analog **1a** (Fig. 1). Analog **1a** was found to have affinity of 0.3 μM for $\alpha_V\beta_3$. The precursor peptide **1a-I** with a free NH_2 group (Fig. 3) was hence acylated with ^{125}I-BH (in the form of its NHS ester), but homology competition assay of the noniodinated peptide **1a** with ^{125}I-**1a** as a tracer

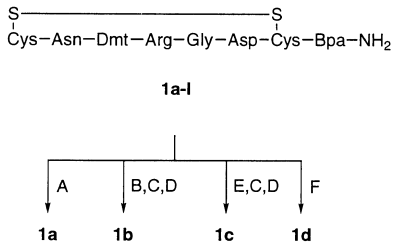

A - 3-(4-phenyl)propanoic acid/DCC/HOBt/DIEA/NMP;
B - Boc-Ahx-NHS/DIEA; C - TFA:DCM:anisol 52:43:5;
D - 3-(3-iodo-4-hydroxyphenyl)propanoic acid NHS/DIEA;
E - Boc-NH-PEG-CO-NHS (MW=3400)/DIEA; F - Biotin-Ahx-(sulfo-NHS)

Figure 3. Modifications at the N-terminus of C-terminal Bpa-containing scaffold **1**.

revealed that the iodinated form did not bind to $\alpha_V\beta_3$. We concluded that either steric hindrance or excessive hydrophobicity was imposed by the bulky and hydrophobic iodine atom.

In order to circumvent these problems, we attempted three different approaches. (i) Insertion of spacers between the iodo-BH group and the RGD 'business part' of the molecule (peptides **1b** and **1c**); (ii) replacement of the radioactive tag by the less hydrophobic, nonradioactive biotin moiety (peptide **1d**); (iii) redesign of the peptide with the radioactive iodine and benzophenone groups moved from the backbone into the ring, which was changed from a disulfide bridge to a phenol-containing lactam (peptide **1j**).

Analogs **1b** and **1c** were prepared in a manner similar to **1a**, but an Ahx or a PEG spacer was inserted, respectively, between the I-BH group and the N-terminal Cys residue (Fig. 3). To allow direct assessment of the binding affinity of iodine-tagged analogs we coupled a nonradioactive I-BH group to the spacer instead of using the noniodinated BH group. Affinity for the $\alpha_V\beta_3$ integrin was measured using the standard radioiodinated echistatin as a tracer by the binding assay described in Experimental Procedures. Peptides **1b** and **1c** had affinities of 0.7 and 0.3 μM, respectively (Fig. 1). Thus, moving the iodine atom away from the RGD triad in peptides based on scaffold **1** restored affinity for the integrin receptor.

Introduction of a biotin group as a tag linked to the N-terminus through an Ahx spacer (Fig. 3) generated peptide **1d**, which had an IC_{50} of 0.5 μM (Fig. 1). By using avidin–horseradish peroxidase or avidin–alkaline phosphatase conjugates as detection systems, the biotin tag could replace the radioactive tag, albeit with a decrease of approximately three orders of magnitude in detection sensitivity.

The third approach attempted to incorporate the photoreactive group and the tag-bearing moiety in the bridging element replacing the original disulfide bridge. A carboxymethylated tyrosine side-chain and the α-amino group were used, respectively, for N- to C-termini cyclization (Fig. 4). In the resulting peptide (**1j**), the benzophenone group was coupled to the α-COOH group of Asp. The modified tyrosine was designed to serve as an incorporation site for the ^{125}I tag. Unfortunately, this peptide showed no affinity for $\alpha_V\beta_3$ even prior to iodination.

We also explored the effect of moving the benzophenone group to two other positions in the scaffold. At the N-terminus, pBz_2OH was coupled either directly (**1e**, **1f**) or through an Ahx spacer (**1g**). A lysine residue was introduced at the C-terminus, and I-BH (**1e**) or biotin (**1f**, **1g**) tags were coupled to its ε-NH_2 group through an Ahx spacer. Analogs **1e**, **1f** and **1g** had IC_{50} values of 1.0, 0.3 and 1.3 μM, respectively (Fig. 1). Replacement of Asn^2 by a substituted Lys residue was still tolerated albeit with somewhat decreased affinity. Coupling of pBz_2OH to the ε-NH_2 group yielded analogs **1h** and **1i** which displayed affinities of 4.5 and 5.6 μM, respectively.

Preparation and binding affinity of cyclic octapeptide analogs of 2

Since close proximity of the ^{125}I tag to the RGD triad appeared at first to abolish affinity for $\alpha_V\beta_3$ (peptide **1a**), we decided to use biotin as a test case in the first design of analogs of scaffold **2**. A Bpa residue was inserted at the C-terminus of **2**, while at the N-terminus the 3-mercaptopropanoic acid (Mpa) was replaced by homocysteine (Hcy) to which biotin was coupled either directly or through an Ahx spacer (Fig. 1). Both peptides **2a** and **2b** showed an unexpected decrease of approximately three orders of magnitude in their affinity for $\alpha_V\mathbf{b}_3$ relative to the unmodified scaffold (Fig. 1). Incorporation of an I-BH group at the N-terminus yielded analog **2c** which, to our surprise, displayed an affinity for the integrin receptor one order of magnitude higher than the biotin-containing analogs (Fig. 1).

Preparation and binding affinity of cyclic pentapeptide analogs of 3

The third scaffold used was the head-to-tail cyclic pentapeptide cyclo[-RGDfV-] [The use of lower case letters in the one letter notation for amino acids indicates D-amino acids.] Keeping the RGD sequence intact, one of the two remaining positions was substituted with either Bpa or N^{ε}-(pBz_2)-Lys as the photoreactive group. The second position was substituted with Tyr as a site for postsynthetic radioiodination. One residue in these two positions was always in a D-configuration. Six of the eight possible permutations were prepared and tested: *cyclo*[-RGD-Bpa-y-], *cyclo*[-RGD-N^{ε}-(pBz_2)-Lys-y-], *cyclo*[-RGDy-N^{ε}-(pBz_2)-Lys-] *cyclo*[-RGD-N^{ε}-(pBz_2)-D-Lys-Y-], *cyclo*[-RGDy-Bpa-] and *cyclo*[-RGDY-N^{ε}-(pBz_2)-D-Lys-] (Fig. 1). A representative synthetic scheme for the preparation of peptide **3b** is shown in Fig. 4. The IC_{50} values observed were between 0.05 and 1.3 μM. The higher range affinities were displayed by the peptides with the D-amino acid next to the aspartic acid as in the unmodified scaffold **3** (Fig. 1). Analog **3c** was the most promising one in this series displaying an IC_{50} of 0.05 μM. This peptide was radioiodinated using the Iodogen® method (52). But as in the

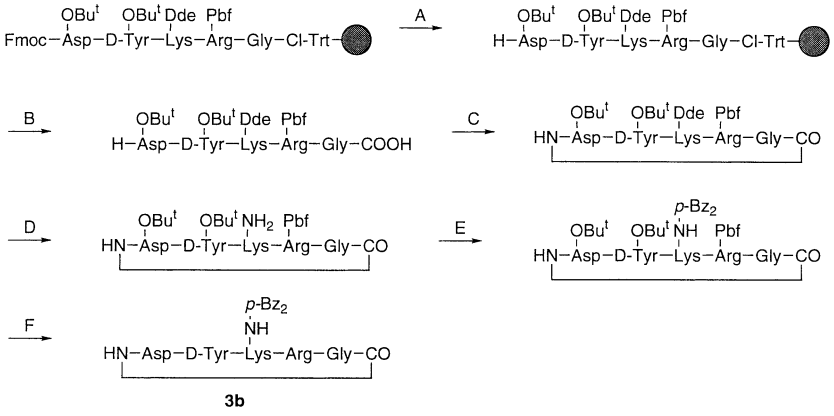

Figure 4. Representative scheme for preparation of the series 3 peptides.

A - 20% piperidin in DMF; B - DCM:TFE:AcOH -3:1:1 ;C - 3 eq. DPPA, 5 eq. $NaHCO_3$/NMP; D - 2% N_2H_4 in DMF; E - 10 eq. *p*-BZ_2OH/DIC/DIEA in DMF; F - TFA:thiocresol:thioanisol:H_2O - 90:55:5:1

case of peptide **1a**, iodination abolished binding to the integrin receptor. In this case, utilization of spacers would not be straightforward. Therefore, we did not further pursue this direction.

Preparation and binding affinity of cyclic hexapeptide analogs of 4

In order to enable derivatization of scaffold **4** by a benzophenone and a tag, the Ser and Pro residues were substituted by L-1,3-diaminopropanoic acid (Dpr) and L-4-aminoproline (Apr), respectively. Selective protection of the Dpr and Apr side-chain amino groups, alternately by Alloc and Dde, enabled selective postsynthetic introduction of the benzophenone group and the tag moiety with or without spacers in either position (Fig. 1). The four analogs in this series showed a 300–700-fold decrease in their affinity for $\alpha_V\beta_3$ relative to the unmodified scaffold. Insertion of an Ahx spacer between the I-BH group and the side-chain of Dpr or Apr caused a slight decrease in affinity. Both analogs containing the Ahx spacer, **4c** and **4d**, showed specific but low efficiency cross-linking to the integrin receptor (Fig. 6).

Preparation of peptidomimetic 5a

The fifth scaffold used was the peptidomimetic **5**. In this molecule the amino group of the Arg residue is methylated and the RGD triad is cyclized through a diphenyl disulfide moiety (Fig. 1). We speculated that the diphenyl disulfide could be replaced by a benzophenone group, thus incorporating the photoreactive moiety into the 'backbone' of the peptidomimetic. Since the benzophenone moiety may impose increased sterical tension on the macrocycle, the Arg residue was not methylated in analog **5a**. Further release of steric constrain was provided by incorporation of a Lys residue, which was inserted in order to provide a 'handle' for introduction of a tag moiety. Interestingly, the molecule was found to be unstable upon storage and underwent considerable decomposition after 2 weeks at 4°C. Some decomposition was observed even when **5a** was stored for longer periods at –20°C. Owing to its low affinity and inherent instability, we did not use in cross-linking experiments.

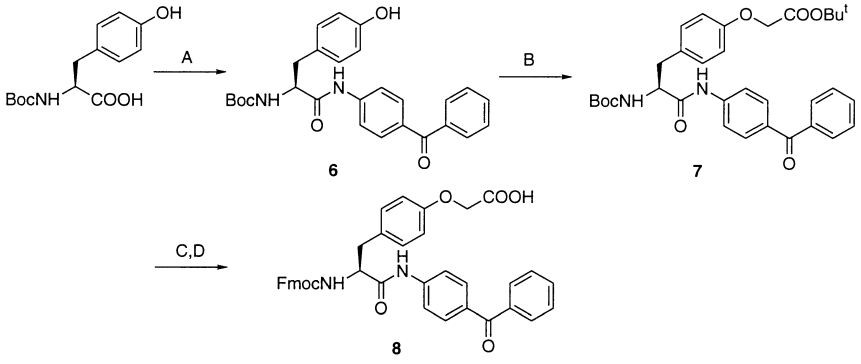

Figure 5. Preparation of Tyr derivative as a building block in the preparation of **1j**.

A - 4-Aminobenzophenone, DCC; B - Br-CH_2COOBu^t, K_2CO_3; C - TFA, scavengers; D - Fmoc-OSu, DIEA

Photoaffinity cross-linking

We further examined the efficiency of those of the photoreactive tagged analogs which displayed affinities in the submicromolar or low micromolar range in cross-linking experiments. ^{125}I-BH-tagged analogs **1b**, **1e**, **1i**, **2c**, **4c** and **4d** were cross-linked to HEK 293 cells expressing a high copy number ($\sim 10^6$) of the $\alpha_V\beta_3$ receptor. All peptides gave specific cross-linking predominantly to the β_3 chain, with the exception of peptide **1i**, which appeared to cross-link to both the α_V and β_3 subunits equally (Fig. 6A). Some nonspecific cross-linking was observed to BSA which was present in the medium. The intensity of this band varied between experiments, but had no effect on the specific cross-linking to the integrin. A large divergence was observed in the specific cross-linking efficiency. For peptides **1i**, **4c** and **4d**, which displayed affinities of 3–7 μM for the receptor, low-efficiency cross-linking was observed. The higher affinity peptides **1b**, **1e** and **2c** cross-linked with high efficiency (Fig. 6A).

Biotin-tagged peptides were cross-linked to purified integrin in solution. The amounts of peptide and receptor used were 2–3 orders of magnitude higher than with the ^{125}I-tagged ligands, in order to compensate for the lower detection sensitivity in this system. Of the four analogs used, the submicromolar affinity possessing **1d** and **1f** gave efficient cross-linking (Fig. 6B), whereas the lower affinity ligands, **1h** and **2a**, gave mainly nonspecific cross-linking which was not competed by the nonlabeled peptide **1** (not shown). In all of the cases where specific cross-linking was observed, it was predominantly ($\geq$ 95%) to the β_3 chain.

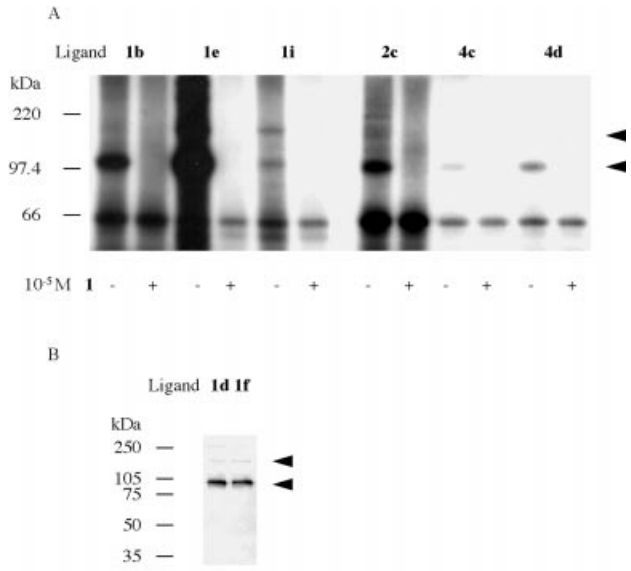

Figure 6. Cross-linking of photoreactive labeled ligands to $\alpha_V\beta_3$. (A) Cross-linking of ^{125}I-labeled peptides to HEK 293 cells expressing high levels of recombinant human $\alpha_V\beta_3$ with or without competition by 10^{-5} M of peptide **1**. The band at M_r 66 kDa is nonspecific cross-linking to BSA which is present in the media. 7.5% SDS–PAGE analysis is visualized by autoradiography. (B) Cross-linking of biotin-tagged peptides to purified $\alpha_V\beta_3$. 7.5% SDS–PAGE/Western blot analysis is visualized by amplified alkaline phosphatase. Size markers (kDa) are shown on the left side of each panel. Arrows indicate the positions of the ligand–β_3 and ligand–α_V conjugates at 100 and 150 kDa, respectively.

Discussion

We have undertaken an effort to use recent advances in photoaffinity cross-linking methodology as a means of elucidating directly the nature of the ligand–$\alpha_V\beta_3$ receptor interface. In contrast to previous cross-linking studies in the integrin field, our objective was not limited to identifying a large fragmentation-restricted domain containing the contact site (contact domain), but rather to generate a detailed map of the surface of the receptor involved in binding by assembling a collection of contact domains, the first of which has recently been identified (41). This domain, β_3[99–118], which cross-links to the benzophenone group at the C-terminus of ligand **1b** may serve as a first constraint in building a three-dimensional model of the integrin–ligand complex.

Our approach to the design of photoreactive tagged peptides for cross-linking was to select highly potent conformationally constrained ligands as scaffolds. These ligands were then modified to incorporate both a benzophenone moiety and either an ^{125}I or a biotin tag. As lead structures, we selected cyclic RGD-containing peptides displaying improved binding affinity relative to their linear counterparts [the later rarely display affinities higher than 10^{-5} M (44)]. We reasoned that by starting with a ligand of high affinity, we could 'afford' to lose some affinity upon modifications involving the introduction of photoreactive and tag moieties, and still obtain ligands which can efficiently and specifically photocross-link.

Since it is practically impossible to accurately predict the combined effects of incorporating both a photoreactive moiety and a reporting 'tag' on binding affinity, we anticipated that only few of the newly designed analogs would be of use in photoaffinity scanning studies. Therefore, five different scaffolds were chosen, modified and assessed in parallel.

Some decrease in binding affinity was found in most of the modified scaffolds. In some cases, no binding was observed after iodine incorporation. Introduction of the bulky iodine

atom into small peptides, such as those used in this study, may confer substantial steric hindrance and/or excessive hydrophobicity, which would result in significant alterations of the peptide conformation. The introduction of two large hydrophobic groups into a relatively small scaffold may result in a hydrophobic collapse of these groups towards each other, and therefore the iodinated peptide may no longer be able to adopt the bioactive conformation (53, 54). In the case of scaffold **1**, this problem could be circumvented by inserting spacers between the iodine-bearing moiety and the RGD pharmacophore. Scaffold **1**, which had the weakest initial binding affinity of the five scaffolds tested, proved to be the most tolerant of structural modifications. Only a moderate decrease in affinity was observed when benzophenone was incorporated at either the N- or the C-terminal regions. Binding affinity was initially lost when an ^{125}I-BH tag was introduced at the N-terminus, but it was restored upon insertion of an Ahx or a PEG spacer between the tag and the N-terminus. Substitution of Asn^2 by Lys followed by modification of the Lys side-chain with a benzophenone group led to analogs **1h** and **1i**, which displayed lower affinities towards $\alpha_V\beta_3$ and in the case of **1i**, low-efficiency cross-linking, respectively. Thus, position 2 of scaffold **1** is less tolerant of substitution by large groups, such as a benzophenone, relative to the N- and C-termini.

The attempt to substitute the disulfide ring by a phenol-containing lactam in analog **1j** was not tolerated, presumably due to an unfavorable conformation of the RGD triad in this rigidified macrocycle.

The influence of the two different tag moieties was found to be case-specific. In contrast to the relatively tolerant scaffold **1**, scaffold **2** was much more sensitive to modifications. The peptides derived from **2** showed 2–3 orders of magnitude lower affinity for the integrin receptor than the original scaffold. The trend of the structure–function relationship displayed by scaffold **2** was reciprocal to that displayed by **1** derivatives. The highest affinity was achieved when an I-BH group was introduced directly at the N-terminus. Replacement of I-BH by biotin yielded a ligand which was 8-fold less potent, and introduction of a spacer between the biotin and the N-terminus reduced the affinity even more. These observations suggest that the close proximity of the I-BH group to the RGD triad in this case may participate in stabilizing the bioactive conformation, or that the biotin group was unfavorably positioned in the receptor-bound state. The benzophenone group in ligand **2c** is introduced as a Bpa at the C-terminus in a position similar to the Bpa residue in **1b**. However, this position is located differently with regard to the RGD triad. Although both scaffolds are essentially heptapeptides with a disulfide bridge between positions 1 and 7, in scaffold **1** the RGD triad is located in the C-terminal end of the ring (positions 4–6), whereas in **2** the RGD occupies positions 2–4 in the N-terminal part of the ring. Future use of **2c** may, thus, provide useful insights which will be incorporated into a receptor–ligand model.

A similar effect of spacer insertion, albeit to a smaller extent, was displayed by the analogs in series **4**. Analogs **4c** and **4d**, in which the I-BH was coupled to the side-chains of Apr and Dpr, respectively, through an Ahx spacer displayed slightly reduced affinities relative to their counterparts, **4a** and **4b**, which did not contain a spacer. Thus, in some cases the closer interaction between the I-BH group and the RGD sequence may be favored over the influences of the long aliphatic chain of the spacer. Additional structural data is required for a more complete understanding of the complex effects of these groups on the bioactive conformation of the RGD pharmacophore.

Scaffold **3** appeared to be moderately tolerant of the substitutions of the favorable D-Phe-Val dipeptide by Tyr and Bpa or ε-(*p*Bz$_2$)-Lys. However, like scaffold **1** it was found to be sensitive to introduction of the bulky and hydrophobic iodine, as evidenced by loss of binding affinity upon radioiodination of ligand **3c**.

The short half-life of ^{125}I compared with the biotin tag represents a drawback. Analysis needs to be performed expeditiously and repeated preparation of the photoreactive radioligand is required. However, the 1000-fold higher sensitivity of detection of the radioactive tag compared with the biotin tag facilitates the monitoring of separation, purification and fragmentation of the photoconjugates after cross-linking. Biotin detection levels can be improved by use of amplification systems, such as the amplified alkaline phosphatase system used in this work, but sensitivity remains inferior to ^{125}I.

In conclusion, we have synthesized new photoreactive, tagged, bioactive RGD-based ligands for the human osteoclast integrin $\alpha_V\beta_3$. Some of these ligands were found capable of efficient and specific cross-linking to the integrin receptor, and will be used in a future systematic program of photoaffinity scanning of the human $\alpha_V\beta_3$ receptor. Using ligand **1b**, we have already identified a 20-amino acid 'contact domain' in the β_3 subunit which contains the cross-linking site for the C-terminus of scaffold **1** (41). We will continue to explore other lead RGD-containing structures as scaffolds for constructing the tools needed for topological mapping of contact sites at the interface between RGD-containing ligands and the integrin receptor.

Acknowledgments: This work was supported in part by Grant AR42833 (to MR) from the National Institutes of Health and by a postdoctoral fellowship (to LS) from the Swiss National Science Foundation. *Cyclo* Ac-[Cys-Asn-Dmt-Arg-Gly-Asp-Cys]-OH was generously provided by Dr S. Rodan, Merck Research Laboratories, West Point, PA.

References

1. Marassi, F.M. & Opella, S.J. (1998) NMR structural studies of membrane proteins. *Curr. Opin. Struct. Biol.* **8**, 640–648.
2. Scherter, G.F., Bartunik, H.D., Michel, H. & Oesterhelt, D. (1993) Orthorhombic crystal form of bacteriorhodopsin nucleated on benzamidine diffracting to 3.6 Å resolution. *J. Mol. Biol.* **234**, 156–164.
3. Kimura, Y., Vassylyev, D.G., Miyazawa, A., Kidera, A., Matsushima, M., Mitsuoka, K., Murata, K., Hirai, T. & Fujiyoshi, Y. (1997) Surface of bacteriorhodopsin revealed by high-resolution electron crystallography. *Nature* **389**, 206–211.
4. Qu, A. & Leahy, D.J. (1995) Crystal structure of the I-domain from the CD11a/CD18 (LFA-1, alpha L beta 2) integrin. *Proc. Natl Acad. Sci. USA* **92**, 10277–10281.
5. Kotzyba-Hibert, F., Kapfer, I. & Goeldner, M. (1995) Recent trends in photoaffinity labeling. *Angew. Chem. Int. Ed. Engl.* **34**, 1296–1312.
6. Zhou, A.T., Bessalle, R., Bisello, A., Nakamoto, C., Rosenblatt, M., Suva, L.J. & Chorev, M. (1997) Direct mapping of an agonist-binding domain within the parathyroid hormone/parathyroid hormone-related protein receptor by photoaffinity crosslinking. *Proc. Natl Acad. Sci. USA* **94**, 3644–3649.
7. Hynes, R.O. (1992) Integrins. Versatility, modulation, and signaling in cell adhesion. *Cell* **69**, 11–25.
8. Stuiver, I. & O'Toole, T.E. (1995) Regulation of integrin function and cellular adhesion. *Stem Cells* **13**, 250–262.
9. Garratt, A.N. & Humphries, M.J. (1995) Recent insights into ligand binding, activation and signalling by integrin adhesion receptor. *Acta Anat.* **154**, 34–45.
10. Ruoslahti, E. (1996) RGD and other recognition sequences for integrins. *Annu. Rev. Cell Dev. Biol.* **12**, 697–715.
11. Brooks, P.C., Strömblad, S., Sanders, L.C., von Schalscha, T.L., Aimes, R.T., Stetler-Stevenson, W.G., Quigly, J.P. & Cheresh, D.A. (1996) Localization of matrix metalloproteinase MMP-2 to the surface of invasive cells by interaction with integrin $\alpha_V\beta_3$. *Cell* **85**, 683–693.
12. Clark, E.A. & Brugge, J.S. (1995) Integrins and signal transduction pathways. The road taken. *Science* **268**, 233–239.
13. Engleman, V.W., Nickols, G.A., Ross, F.P., Horton, M.A., Griggs, D.W., Settle, S.L., Ruminski, P.G. & Teitelbaum, S.L. (1997) A peptidomimetic antagonist of the $\alpha_V\beta_3$ integrin inhibits bone resorption *in vitro* and prevents osteoporosis *in vivo*. *J. Clin. Invest.* **99**, 2284–2292.
14. Horton, M.A. (1997) The $\alpha_v\beta_3$ integrin 'vitronectin receptor'. *Int. J. Biochem. Cell Biol.* **29**, 721–725.
15. Yamamoto, M., Fisher, J.E., Gentile, M., Seedor, J.G., Leu, C.-T., Rodan, S.B. & Rodan, G.A. (1998) The integrin ligand echistatin prevents bone loss in ovariectomized mice and rats. *Endocrinology* **139**, 1411–1418.
16. Loftus, J.C., O'Toole, T.E., Plow, E.F., Glass, A., Frelinger 3rd, A.L. & Ginsberg, M.H. (1990) A beta 3 integrin mutation abolishes ligand binding and alters divalent cation-dependent conformation. *Science* **249**, 915–918.
17. Bajt, M.L. & Loftus, J.C. (1994) Mutation of ligand binding domain of beta 3 integrin. Integral role of oxygenated residues in alpha IIb beta 3 (GPIIb-IIIa) receptor function. *J. Biol. Chem.* **269**, 20913–20919.
18. Tozer, E.C., Liddington, R.C., Sutcliffe, M.J., Smeeton, A.H. & Loftus, J.C. (1996) Ligand binding to integrin $\alpha_{IIb}\beta_3$ is dependent on a MIDAS-like domain in the β_3 subunit. *Cell* **79**, 659–667.
19. Takagi, J., Kamata, T., Meredith, J., Puzon-McLaughlin, W. & Takada, Y. (1997) Changing ligand specificities of $\alpha_V\beta_1$ and $\alpha_V\beta_3$ integrins by swapping a short diverse sequence of the β subunit. *J. Biol. Chem.* **272**, 19794–19800.
20. Lin, E.C.K., Ratnikov, B.I., Tsai, P.M., Carron, C.P., Myers, D.M., Barbas III, C.F. & Smith, J.W. (1997) Identification of a region in the integrin β_3 subunit that confers ligand binding specificity. *J. Biol. Chem.* **272**, 23912–23920.
21. Peterson, J.A., Visentin, G.P., Newman, P.J. & Aster, R.H. (1998) A Recombinant soluble form of the integrin $\alpha_{IIb}\beta_3$ (GPIIb-IIIa) assumes an active, ligand-binding conformation and is recognized by GPIIb-IIIa-specific monoclonal, allo-, auto, and drug-dependent platelet antibodies. *Blood* **92**, 2053–2063.
22. D'Souza, S.E., Haas, T.A., Piotrowicz, R.S., Byers-Ward, V., McGrath, D.E., Soule, H.R., Cierniewski, C., Plow, E.F. & Smith, J.W. (1994) Ligand and cation binding are dual functions of a discrete segment of the integrin beta 3 subunit: cation displacement is involved in ligand binding. *Cell* **79**, 659–667.
23. Pelletier, A.J., Kunicki, T. & Quaranta, V. (1996) Activation of the integrin $\alpha_V\beta_3$ involves a discrete cation-binding site that regulates conformation. *J. Biol. Chem.* **271**, 1364–1370.
24. D'Souza, S.E., Ginsberg, M.H., Burke, T.A., Lam, S.C.-T. & Plow, E.F. (1988) Localization of an Arg-Gly-Asp recognition site within an integrin adhesion receptor. *Science* **242**, 91–93.
25. Smith, J.W. & Cheresh, D.A. (1988) The Arg-Gly-Asp binding domain of the vitronectin receptor. photoaffinity cross-linking implicates amino acid residues 61–203 of the β subunit. *J. Biol. Chem.* **263**, 18726–18731.
26. Calvete, J.J., McLane, M.A., Stewart, G.J. & Niewiarowski, S. (1994) Characterization of the cross-linking site of disintegrins albolabrin, bitistatin, echistatin and eristostatin on isolated human platelet integrin GPIIb/IIIa. *Biochem. Biophys. Res. Commun.* **202**, 135–140.
27. Weber, P.J. & Beck-Sickinger, A.G. (1997) Comparison of the photochemical behavior of four different photoactivable probes. *J. Peptide Res.* **49**, 375–383.
28. Taylor, M.F., Bhatacharyya, A.K., Rajagopalan, K., Hiipakka, R., Liao, S. & Collins, D.C. (1996) Photoaffinity labeling of rat steroid 5 alpha-reductase (isozyme-1) by a benzophenone derivative of a 4-methyl-4-azasteroid. *Steroids* **61**, 323–331.
29. Wang, J., Bauman, S. & Colman, R.F. (1998) Photoaffinity labeling of rat liver glutathione *S*-rransferase, 4-4, by glutathionyl *S*-[4-(succinimidyl)-benzophenone]. *Biochemistry* **37**, 15671–15679.
30. Macdonald, S.G., Dumas, J.J. & Boyd, N.D. (1996) Chemical cross-linking of the Substance P (NK-1) receptor to the a subunits of the G Proteins G_q and G_{11}. *Biochemistry* **35**, 2909–2916.

31. Wilson, C.J., Husain, S.S., Stimson, E.R., Dangott, L.J., Miller, K.W. & Maggio, J.E. (1997) *p*-(4-Hydroxybenzoyl) phenylalanine: a photoreactive amino acid analog amenable to radioiodination for elucidation of peptide–protein interaction. Application to substance P receptor. *Biochemistry* **36**, 4542–4551.
32. Bisello, A., Mierke, D.F., Pellegrini, M., Rosenblatt, M., Suva, L.J. & Chorev, M. (1998) Parathyroid hormone–receptor interactions identified directly by photocrosslinking and molecular modeling studies. *J. Biol. Chem.* **273**, 22498–22505.
33. Mannstadt, M., Luck, M.D., Gardella, T.J. & J.Ÿppner, H. (1998) Evidence for a ligand interaction site at the amino-terminus of the parathyroid hormone (PTH)/PTH-related protein receptor from cross-linking and mutational studies. *J. Biol. Chem.* **273**, 16890–16896.
34. Ploug, M., Ostergaard, S., Hansen, L.B., Holm, A. & Dano, K. (1998) Photoaffinity labeling of the human receptor for urokinase-type plasminogen activator using a decapeptide antagonist. Evidence for a composite ligand-binding site and a short interdomain separation. *Biochemistry* **37**, 3612–3622.
35. Bernier, S.G., Bellemare, J.M.L., Escher, E. & Guillemette, G. (1998) Characterization of AT4 receptor from bovine aortic endothelium with photosensitive analogues of angiotensin IV. *Biochemistry* **37**, 4280–4287.
36. Dong, M., Wang, Y., Pinon, D.I., Hadac, E.M. & Miller, L.J. (1999) Demonstration of a direct interaction between residue 22 in the carboxyl-terminal half of secretin and the amino-terminal tail of the secretin receptor using photoaffinity labeling. *J. Biol. Chem.* **274**, 903–909.
37. Mullen, D.G., Cheng, S., Ahmed, S., Blevitt, J.M., Bonnin, D., Craig, W.S., Ingram, R.T., Mazur, C., Minasyan, R., Tolley, J.O., Tschopp, J.F., Pierschbacher, M.D. (1996) Development of peptide antagonists of the integrin $\alpha_v\beta_3$. In *Peptides: Chemistry, Structure and Biology* (Kaumaya, P.T.P. & Hodges, R.S., eds). Mayflower Scientific Ltd, Kingswinford, UK, pp. 207–208.
38. Pfaff, M., Tangemann, K.M., Ÿller, B., Gurrath, M.M., Ÿller, G., Kessler, H. & Timpl, R. (1994) Selective recognition of cyclic RGD peptides of NMR defined conformation by alpha IIb beta 3, alpha V beta 3, and alpha 5 beta 1 integrins. *J. Biol. Chem.* **269**, 20233–20238.
39. Ali, F.E. & Samanen, J.M. (1991) Synthesis of protected cyclic homodetic peptides by solid phase peptide synthesis. In *Innovations and Perspectives in Solid Phase Synthesis & Related Technologies.* (Epton, R., ed.). DPCC (UK) Ltd, London, pp. 333–335.
40. Keenan, R.M., Miller, W.H., Kwon, C., Ali, F.E., Callahan, J.F., Calvo, R.R., Hwang, S.-M., Kopple, K.D., Peishoff, C.E., Samanen, J.M., Wong, A.S., Yuan, C.-K. & Huffman, W.F. (1997) Discovery of potent nonpeptide vitronectin receptor ($\alpha_V\beta_3$) antagonists. *J. Med. Chem.* **40**, 2289–2292.
41. Bitan, G., Scheibler, L., Rosenblatt, M. & Chorev, M. (1999) Mapping the integrin $\alpha_V\beta_3$-ligand interface by photoaffinity crosslinking. *Biochemistry* **38**, 3414–3420.
42. Behar, V., Nakamoto, C., Greenberg, Z., Bisello, A., Suva, L.J., Rosenblatt, M. & Chorev, M. (1996) Histidine at position 5 is the specificity 'switch' between two parathyroid hormone receptor subtypes. *Endocrinology* **137**, 4217–4224.
43. Suva, L.J., Flannery, M.S., Caulfield, M.P., Findlay, D.M.J., Ÿppner, H., Goldring, S.R., Rosenblatt, M. & Chorev, M. (1997) Design, synthesis and utility of novel benzophenone-containing calcitonon analogs for photoaffinity labeling the calcitonin receptor. *J. Pharmacol. Exp. Ther.* **283**, 876–884.
44. Wermuth, J., Goldman, S.L., Jonczyk, A. & Kessler, H. (1997) Stereoisomerism and biological activity of the selective and super-active $\alpha_V\beta_3$-integrin inhibitor cyclo (-RGDfV-) and its retro-inverso peptide. *J. Am. Chem. Soc.* **119**, 1328–1335.
45. Loffet, A. & Zhang, H.X. (1993) Allyl-based groups for side-chain protection of amino acids. *Int. J. Peptide Protein Res.* **42**, 346–351.
46. Abraham, D.J., Mokotoff, M. & Simmons, J.E. (1983) Design, synthesis, and testing of antisickling agents. 2. Proline derivatives designed for the donor site. *J. Med. Chem.* **26**, 594–554.
47. McCafferty, D.G., Slate, C.A., Nakhle, B.M., Graham, H.D., Austell, T.L., Vachet, R.W., Mullis, B.H. & Erickson, B.W. (1995) Engineering of a 129-residue tripod protein by chemoselective ligation of proline-II helixes. *Tetrahedron* **51**, 9859–9872.
48. Kaduk, C., Wenschuh, H., Beyermann, M., Forner, K., Carpino, L.A. & Bienert, M. (1995) Synthesis of Fmoc-amino acid fluorides via DAST, an alternative fluorinating agent. *Lett. Peptide Sci.* **2**, 285–288.
49. Carpino, L.A. & El-Faham, A. (1995) Tetramethylfluoroformamidinium hexafluorophosphate: a rapid-acting peptide coupling reagent for solution and solid phase peptide synthesis. *J. Am. Chem. Soc.* **117**, 5401–5402.
50. Greenberg, Z., Stoch, S.A., Traianedes, K., Teng, H., Suva, L.J., Rosenblatt, M. & Chorev, M. (1999) Covalent immobilization of recombinant human $\alpha_V\beta_3$ integrin on a solid support with retention of functionality. *Anal. Biochem.* **266**, 153–164.
51. Matsudaira, P. (1987) Sequence from picomole quantities of proteins electroblotted onto polyvinylidene difluoride membranes. *J. Biol. Chem.* **262**, 10035–10038.
52. Roubini, E., Doung, L.T., Gibbons, S.W., Leu, C.-T., Caulfield, M.P., Chorev, M. & Rosenblatt, M. (1992) Synthesis of fully active biotinylated analogues of parathyroid hormone and parathyroid hormone-related protein as tools for the characterization of parathyroid hormone receptors. *Biochemistry* **31**, 4026–4033.
53. Kurz, M. & Guba, W. (1996) 3D Structure of ramoplanin: a potent inhibitor of bacterial cell wall synthesis. *Biochemistry* **35**, 12570–12575.
54. Ilyina, E. & Mayo, K.H. (1995) Multiple native-like conformations trapped via self-association-induced hydrophobic collapse of the 33-residue beta-sheet domain from platelet factor 4. *Biochem. J.* **306**, 407–419.